JJMIE

Volume 18, Number 4, December. 2024
ISSN 1995-6665
Pages 645- 652
https://doi.org/10.59038/jjmie/180401
Editor-in-Chief: Prof. Ali M. Jawarneh

Jordan Journal of Mechanical and Industrial Engineering

Characterization studies on various green synthesized nanoparticles for photovoltaic solar panel applications

Priya Palanichamy[1*], Rajesh Krishnasamy[1], Senthil Muthu Kumar Thiagamani[2,3,4*], Pavitra Rajendran[5], R.A. Ilyas[4,6], Choon Kit Chan[3]

[1]*Department of Electrical and Electronics Engineering, Kalasalingam Academy of Research and Education, Krishnan Koil 626126, Tamil Nadu, India.*
[2]*Department of Mechanical Engineering, Kalasalingam Academy of Research and Education, Anand Nagar, Krishnankoil 626126, Tamil Nadu, India.*
[3]*Department of Mechanical Engineering, Faculty of Engineering and Quantity Surveying, INTI International University, Putra Nilai, 71800 Nilai, Negeri Sembilan, Malaysia.*
[4]*Centre for Advanced Composite Materials (CACM) Universiti Teknologi Malaysia, 81310 Skudai, Johor Bahru, Johor, Malaysia.*
[5]*Center for Supramolecular Chemistry, Department of Chemistry, KalasalingamAcademy of Research & Education, Krishnan Koil 626126, Tamil Nadu, India.*
[6]*Department of Chemical Engineering, Faculty of Chemical and Energy Engineering, Universiti Teknologi Malaysia, 81310 UTM, Johor, Malaysia.*

Received 25 Feb 2024 *Accepted 10 Aug 2024*

Abstract

The green nanotechnology field has received ample attention and emerged as a viable option for producing nanoparticles (NPs) in an eco-friendly, sustainable, and reliable manner. The rosy periwinkle leaf extract to metal oxide NPs is an encouraging alternative to chemical synthesis. In this study, aluminum (Al), copper (Cu), and zinc oxide (ZnO) nanoparticles (NPs) synthesized using a sustainable technique to evaluate their electrical conductivity and characterized by X-ray diffraction (XRD), ultraviolet-visible (UV-vis), Fourier-transform infrared spectroscopy (FTIR), scanning electron microscopy (SEM), and energy dispersive X-ray spectroscopy (EDX) to determine the crystalline structures and optical properties, functional groups, surface morphology, and elemental compositions of NPs. XRD peaks confirmed that the Al, ZnO were structurally crystalline whereas copper peaks were absorbed as amorphous. In UV-visible spectroscopy, the surface plasmon resonance of NPs is observed at peaks of 237nm, 328nm, and 363nm. FTIR spectra of AlNPs, CuNPs, and ZnNPs were analyzed, revealing distinctive peaks for each. AlNPs showed O-H stretching and carbon group vibrations, CuNPs exhibited carbon and halo compound stretching, and ZnNPs displayed isothiocyanate and carbon group stretching along with metal oxide vibrations. An electrical conductivity test showed that NPs were excellent electrical conductors, making them suitable for photovoltaic solar panel coatings. Thus, Al, Cu, and Zn NPs can used for photovoltaic solar panel coating applications to improve electrical conductivity.

Keywords: Green synthesis, Nanoparticles, Characterization, Electrical Conductance.

1. Introduction

Nanoparticles are tiny particles with dimensions typically in the range of 1 to 100 nanometres (nm). Metal NPs, namely ZnO, Cu, and Al, have garnered interest recently due to their crucial coating characteristics that enhance solar cell performance. NPs are intentionally designed and synthesized to create functional materials with specific properties for various applications [1-3]. Previous studies have shown that changing the size, shape, and arrangement of nanoparticles in devices can greatly improve how well they work. Green synthesis refers to the process of using plants or plant parts to reduce metal ions to their elemental form, creating metal NPswith sizes ranging from 1 to 100 nanometers. Compared to traditional methods, this approach is more efficient, simpler, and cheaper. It can also be easily scaled up for larger operations. Green synthesis of NPs is a safe and cost-effective way to address environmental pollution. It focuses on creating sustainable methods that avoid harmful byproducts. Using plant extracts is one of the most eco-friendly ways to produce metal oxide NPs. This method is generally easier and more practical for large-scale production than using bacteria or fungi. Microorganisms or plant extracts, are employed in green synthesis to create nanoparticles. The plant extract was combined with a metal salt solution for the environmentally friendly production of metal nanoparticles [4]. It involves combining phytochemicals from plant extracts in various combinations and concentrations, as well as other factors such as pH. The electrochemical potential and biological reduction potential of a metal ion may be

* Corresponding author e-mail: tsmkumar@klu.ac.in; priya.p@klu.ac.in.

ascertained by analyzing its temperature, concentration, pressure, and reaction time[22-23]. When metal ions change from their mono valent or divalent state to a zero-valent state, metal nanoparticles are created.

Compared to alternative chemical and physical processes, the green synthesis of metal nanoparticles offers benefits including lower toxicity, a one-step procedure, cost-effectiveness, environmental friendliness, and the absence of the need for further capping or stabilizing chemicals. Different plant parts, such as roots, stems, latex, leaves, and seeds, are utilized for the synthesis of metal NPs.

While traditional physical and chemical methods for making nanoparticles (NPs) have been used for years, they often create harmful byproducts that can damage the environment [24-25]. To address these issues, the bottom-up approach in green synthesis has been developed as an eco-friendly alternative to these traditional techniques.

Green Tea, Aloe vera, Neem (*Azadirachta indica*), Tulsi (*Ocimum sanctum*), Moringa oléifera, and Grape extracts have all been used to demonstrate the green synthesis of Al NPs. Earlier studies reported that Cu NPs were synthesized from various types of plants such as fire lily (*Gloriosa superba L.*), common grape (*Vitis vinifera*, *Nerium*), Nerium (*Nerium oleander*), Ceylon caper (*Capparis zeylanica*), and Jackfruit-Champa (*Artabotrysodoratissimus*), Magnolia (*Nag Champa*) (*ArtabotrysOdoratissimus*) and Angel's trumpet (*Datura innoxia*).The green synthesis of ZnO NPs has been shown utilizing several plant extracts, including *Lobelia leschenaultiana*, *Agathosmabetulina*, *Laurus nobilis*, *Moringa olifera*, *Acalypha indica*, *Aspalathus linearis*, *Carica papaya*, green tea leaves, *Euphorbia jatropha latex*, *Andrographis paniculata*, *Chamaecostuscuspidatus*, and mango seed extracts [5-8].

Metal nanoparticles have diverse applications, including catalysis, drug delivery, and various biomedical fields. The green-synthesized NPs were characterized using X-ray diffraction (XRD), ultraviolet-visible (UV-vis) spectroscopy, Fourier-transform infrared spectroscopy (FTIR), scanning electron microscopy (SEM), and energy-dispersive X-ray spectroscopy (EDX) [26-27]. XRD investigates structural properties to determine structural parameters and crystallite size. In the future, the green synthesis of NPs such as Al, Cu, and ZnO using rosy periwinkle leaf extract can be used for photovoltaic solar panel coating applications [9].

2. Materials and Methods

2.1. Collection of Plant leaves

Fresh rosy periwinkle leaves were collected from the agricultural farm at Kalasalingam Academy of Research and Education in Krishnankoil, Tamil Nadu, India. Ethanol was used as a solvent for extracting bioactive compounds from the rosy periwinkle leaves. Hydrochloric acid (HCl) and sodium hydroxide (NaOH) were employed for pH adjustments. pH is an important parameter in many chemical reactions and can influence the characteristics of the synthesized NPs [10]. Aluminum chloride ($AlCl_3$), copper sulphate ($CuSO_4$), and zinc nitrate ($Zn(NO_3)_2$) were used as metal salts. These salts provided metal ions necessary for the synthesis of Al, Cu, and Zn NPs. A centrifuge (REMI-R8C, Laboratory Instruments, India) was used to separate solid particles from the rosy periwinkle leaves extract, and stirring of the rosy periwinkle extract was performed using a magnetic stirrer (REMI-MH2, Laboratory Instruments, India)

2.2. Green Synthesis of Nanoparticles

The synthesis of Al, Cu, and Zn NPs was carried out using rosy periwinkle leaf extracts according to the method described by Huang, Weng, Chen, Megharaj, and Naidu with some modifications

2.2.1. Preparation of rosy periwinkle leaf extract

800 grams of fresh rose periwinkle leaves were twice cleaned with distilled water and allowed to dry for a full day. The leaves were dried, then chopped into small bits and brought to a boil in one litre of double-distilled water for half an hour. The solution was filtered using Whatman No. 1 filter paper once it had cooled. The leaf extract filtrate was collected in a beaker and kept cold (4°C) for later use.

2.2.2. Preparation of reagents

1M solution of $AlCl_3$, $CuSO_4$, and $Zn(NO_3)_2$ solution was prepared and labelled as stock. Different concentrations (1mM, 2mM, 10mM, and 20mM) of $AlCl_3$, $CuSO_4$, and $Zn(NO_3)_2$ was prepared from the stock solutions.

2.2.3. Synthesis of Al NPs

To ensure proper mixing of the solution, the prepared extract was combined with a saturated solution of aluminum chloride and placed in a magnetic stirrer for two hours. Following the stirring process, the pH was measured to monitor the reaction between the extract's phytochemicals and the metal ions that produced the metal oxide nanoparticles. After using a cooling centrifuge to settle down the leftover extract, the reaction mixture was centrifuged at 2500 rpm for 20 minutes. The resulting supernatant was then ultra-centrifuged for another 30 minutes at 14,000 rpm. After discarding the resultant supernatant, the pellets underwent several water and ethanol washes before being dried at 60 °C in a hot air oven to produce Al_2O_3 NPs.

2.2.4. Synthesis of Cu NPs

The rosy periwinkle was used to create Cu NPs by combining $CuSO_4$ solution with leaf extract. To put it briefly, 1 mmol/L of $CuSO_4$ and 4:1 volumetric ratio of leaf extract was added, and the mixture was continuously stirred for 10 minutes at 80˚ C. After allowing the reaction to finish at room temperature for a full day, the resultant suspensions were separated according to the previously described methodology. Following incubation, copper nanoparticles were found to become green instead of blue.

2.2.5. Synthesis of ZnO NPs

2 grams of zinc nitrate were added to 42.5 ml of each extract to create the ZnO NPs. Following a 60-minute stirring period, these mixes were submerged in a 60-minute water bath heated to 60 degrees Celsius. The mixes were then heat-treated for an hour at 400 °C after being dried at 150 °C.

2.3. Characterization studies

All of the synthesized NPs' structural, functional, and optical characteristics were assessed using an energy-dispersive x-ray (EDX), UV/Vis, Fourier-transform infrared (FTIR), and Scanning Electron Microscopy (SEM).

2.3.1. X-ray Diffraction

XRD may be used to examine the atomic structures of materials [11]. To distinguish between the qualitative and quantitative levels of materials, this system is useful. The size and structure of the crystalline nanoparticles were identified and verified using XRD analysis. A Bruker (D8 advance ECO, Germany) diffractometer was used to analyze the produced sample of nanoparticles using X-rays with a wavelength of (λ) = 1.54056 Å. The diffractometer was operated at a voltage of 40 kV and a current of 35 mA. To account for the crystalline structure, the acquired pictures were compared with the Joint Committee on Powder Diffraction Standards (JCPDS) collection. Using an X-ray diffractometer, X-ray diffraction patterns were acquired in the 10-800 range at a scan rate of 40/min.

2.3.2. Fourier Transform Infrared Analysis

An IR spectrometer operating in reflection mode was used to record the metal nanoparticles' FTIR spectra [12]. After centrifuging the generated Al, Cu, and ZnO NPs from the rosy periwinkle extract for 20 minutes at 10,000 rpm, the pellet was cleaned three times using distilled water. After that, it is dried for a whole day at 60°C in an oven. FTIR spectra of FA samples were obtained using an FTIR spectrometer with a nominal resolution of 2 cm^{-1}, covering the range of 4000–400 cm^{-1}.

2.3.3. Ultraviolet-visible spectrometer analysis

The primary method and simplest approach to verify nanoparticle production is UV-Vis spectroscopy [13]. Using purified water as a reference, the absorption spectrum of the colloidal sample was measured with a UV-Vis spectrometer (Systronics 306, India) in the 200–800 nm range. The metal nanoparticles' UV-Vis spectra were used to track the reduction of Al, Cu, and Zn ions.

2.3.4. Morphological Analysis

A scanning electron microscope of ZEISS-EVO 18, equipped with EDX (EDAX -APEX) & mapping was used to investigate the morphology of ZnO, Cu, and Al NPs. SEM may be used to characterize NPs [14].This instrumentation experiment aims to determine the dispersion, morphology, size, and form of artificial nanoparticles. One strong analytical method that is frequently used to ascertain the elemental composition of materials, including nanoparticles, is energy-dispersive X-ray spectroscopy (EDX). For EDX to function, a sample must be exposed to high-energy X-rays for it to release distinctive X-rays. The elements contained in the sample may be identified since the energy of these X-rays is related to the element's atomic number. When it comes to NPs, EDX is especially helpful for determining the elemental makeup of nanoparticles that are derived from natural sources.

2.3.5. Conductivity test

Conductance was measured from a digital conductivity meter (Systronics-MK 509, India) with a standard of 0.01NKcl unit S/m [15]. The green synthesized NPs samples such as Al, Cu, Zn, and Ag were measured by electrodes of the conductivity meter after calibration with a standard solution. Conductivity testing should be done three times to ensure the correctness of each NP sample.

3. Results and Discussions

3.1. X-Ray Diffraction Analysis

The crystalline nature of Al and Zn NPs was investigated using X-ray diffraction. The diffraction pattern, recorded within the 2θ range of 100 to 800, is depicted in Fig. 1. XRD patterns confirm the presence of crystalline phases in the Al samples. The diffraction peaks of Al were identified at 2θ values of 31.860, 45.500, 56.500, 66.500, 75.330, and 84.030, corresponding to the crystalline planes of (220), (223), (205), (602), (604), and (623), respectively. This confirms that the prepared Al possesses a body-centered cubic structure (JCPDS no: 2-0545) [16]. Similarly, XRD patterns validate the presence of crystalline phases in Zn NP samples. XRD patterns confirm the presence of amorphous nature in Cu nanoparticles as shown in Fig 1. The diffraction peaks of Zn NPs were observed at 2θ values of 31.790, 34.350, 36.210, 47.810, 56.530, 62.820, 67.870, and 72.720, corresponding to the crystalline planes of (100), (002), (101), (102), (110), (103), (112), and (202), respectively. This confirms that the prepared Zn NPs possess a body-centered cubic structure (JCPDS no: 79-0208)[17].

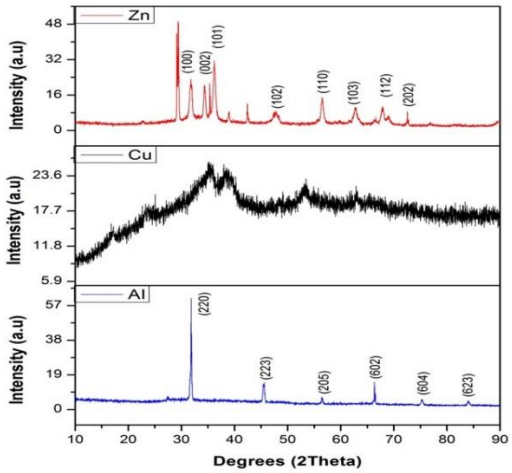

Figure 1. X-ray diffraction pattern of synthesized Al, Cu, Zn NPs

3.2. Fourier Transform Infrared Analysis (FTIR)

The FTIR spectra of AlNPs, CuNPs, and ZnNPs are illustrated in Fig. 2. The O-H stretching peaks for the hydroxyl molecules are observed at 3410.82, 3444.87, and 3432.47 cm^{-1} for AlNPs, CuNPs, and ZnNPs, respectively. In the FTIR spectrum of AlNPs, broad peaks at 1901.81 and 1078.21 cm^{-1} correspond to the stretching vibrations of C-H and C-N in the carbon groups. A sharp peak at 1111 cm^{-1} indicates S=O stretching in sulfonyl chloride. Peaks at 584.43 cm^{-1} represent the C-Br and C-I stretching in halo

compounds. For CuNPs, the FTIR spectrum exhibits broad peaks at 1633.71 and 1384.89 cm^{-1}, representing the stretching vibrations of C=O and C-H in carbon groups. A sharp peak at 1111 cm^{-1} indicates C-F stretching in fluoro compounds. Peaks at 619.15 and 518.85 cm^{-1} represent the C-Br and C-I stretching in halo compounds. The sharp peak at 428.20 cm^{-1} in the fingerprint region is attributed to metal oxide vibration modes, specifically Cu-O vibrations. In the case of ZnNPs, the FTIR spectrum shows a broad peak at 2092.77 cm^{-1}, signifying the N=C=S stretching of the isothiocyanate compound. Other broad peaks at 2434.17 cm^{-1} indicate O=C=O stretching of carbon dioxide. A sharp peak at 1637.56 cm^{-1} suggests N-H bending. Peaks at 1793.80, 1381.03, and 835.18 cm^{-1} represent the stretching vibrations of C=O, C=H, and C=C in the carbon groups, respectively [18].

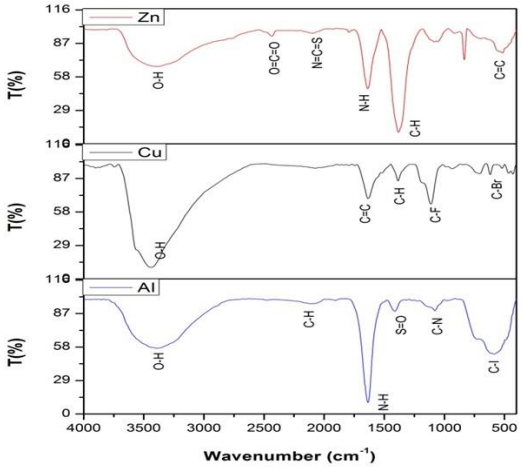

Figure 2. Fourier Infra-red (FTIR) Spectrum of synthesized Al, Cu, and Zn NPs

3.3. Ultraviolet-Visible Spectrometer Analysis

A comparative study was conducted to examine the UV-visible spectrum of Al, Cu, and Zn NPs in Table 1 and Fig. 3. The absorbance peak was recorded from the 200 to 800 nm range in the UV UV-visible spectrum of Al, Cu, and Zn NPs. The binary metal of prepared Al NPs was confirmed by the presence of a single broad absorption peak at 237 nm attributed to aluminum-oxygen interaction. At the same time, the prepared Cu NPs confirmed by the wider absorption peak at 328 nm due to the copper-oxygen interaction. Furthermore, because of the zinc-oxygen interaction, the produced Zn NPs contact was verified by the absorbance peak range of 363 nm. In nano ranges, the size of Al, Cu, and Zn NPs was represented by this wide peak. Based on the above results, the prepared Al, Cu, and Zn NPs have good optical properties with a photo adjustment in the spectrum of the UV-visible region. Furthermore, free electrons present in green synthesized metal nanoparticles produce a surface plasmon resonance absorption band as a result of the metal nanoparticles' electrons mutually vibrating in resonance with light waves. The peaks' appearances demonstrated the features of the NPs' surface plasmon resonance [19].

Table 1. UV spectra of Al, Cu, and Zn NPs

Nanoparticles	Wavelength (nm)
Al_2O_3	237
Cu_2O	328
ZnO	363

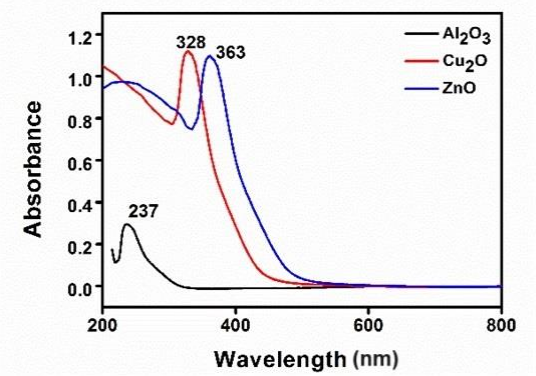

Figure 3. UV spectra of Al NPs, Cu NPs, and Zn NPs

3.4. Morphological Analysis

The morphology of aluminum (Al), copper (Cu), and zinc (Zn) nanoparticles (NPs) was investigated through scanning electron microscopy (SEM), as depicted in Figure 4. The surface characteristics of Al, Cu, and Zn NPs were examined at various magnifications. The SEM image illustrates a cubic shape, as shown in (Fig. 4 a, b). In the case of Cu NPs, the structural analysis revealed the presence of a combination of spherical-shaped particles and a few aggregates, attributed to the coating of various surface functional groups from the plant extract, as evidenced in (Fig. 4c, d). Morphological analysis conducted through SEM indicated that Zn NPs displayed cubic-shaped structures, as illustrated in (Fig. 4e,f) Figure.4. presents a comprehensive morphological characterization of aluminum (Al), copper (Cu), and zinc oxide (Zn) nanoparticles (NPs) using scanning electron microscopy (SEM). (a-b), the arrow marks indicate that Al NPs exhibit cubic shapes; (c-d) illustrate the morphology of Cu NPs, and (e-f) depict the morphology of Zn NPs. The arrow marks in both (c-d) and (e-f) emphasize the cubic-shaped structures of Cu and Zn NPs, respectively[20].

3.5. EDX Analysis

EDX analysis was utilized to determine the elemental composition of Al NPs, Cu NPs, and Zn NPs. The findings revealed a predominant presence of oxygen (O) and aluminum (Al) in the Al NPs. Interestingly, the inclusion of Al NPs introduced a higher concentration of aluminum (Al) as an additional element, illustrated in Fig. 5(i) (a-e), Specifically, Al contributed to 24.7%, while O contributed to 75.3% of the total atomic weight in Al NPs. Similarly, EDX analysis demonstrated the presence of oxygen (O) and copper (Cu) in Cu NPs. Remarkably, the incorporation of Cu NPs introduced an elevated concentration of copper (Cu) as an additional element, depicted in Fig. 5(ii) a-e. Specifically, Cu contributed to 17.8%, while O contributed to 82.2% of the total atomic weight in Cu NPs. Furthermore,

the EDX analysis findings highlighted a predominant presence of oxygen (O) and zinc (Zn) in Zn NPs. Interestingly, the inclusion of Zn NPs introduced a heightened concentration of zinc (Zn) as an additional element, as shown in Fig. 5(iii) (a-e). Specifically, Zn contributed to 26.6%, while O contributed to 73.4% of the total atomic weight in Zn NPs. This elemental analysis underscores the successful integration of Al, Cu, and Zn NPs into the synthesized nanoparticles using different approaches, confirming the efficacy of the fabrication methods [21].

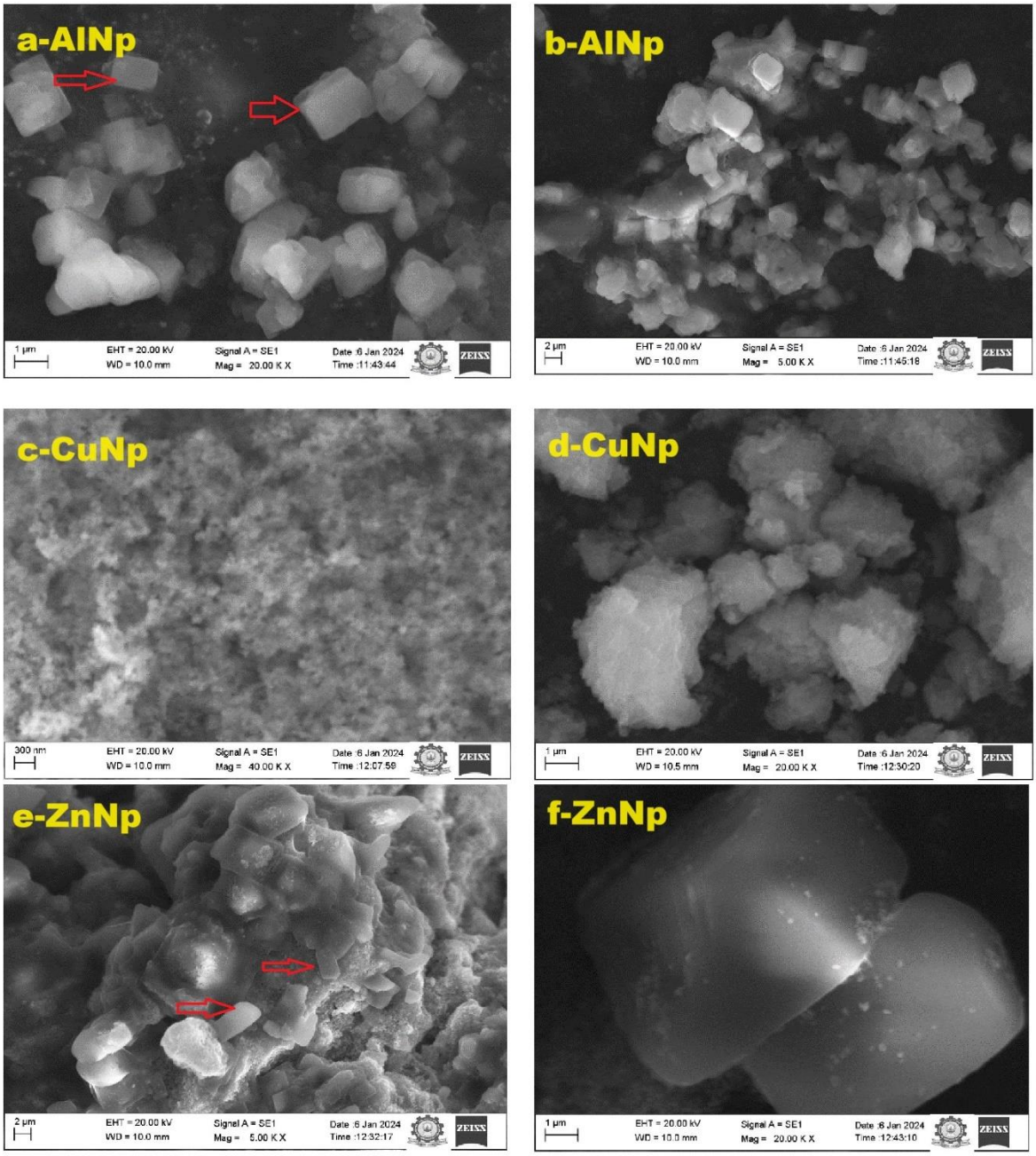

Figure 4. (a-f): SEM Microscopic image of Al NPs, Cu NPs, and Zn NPs

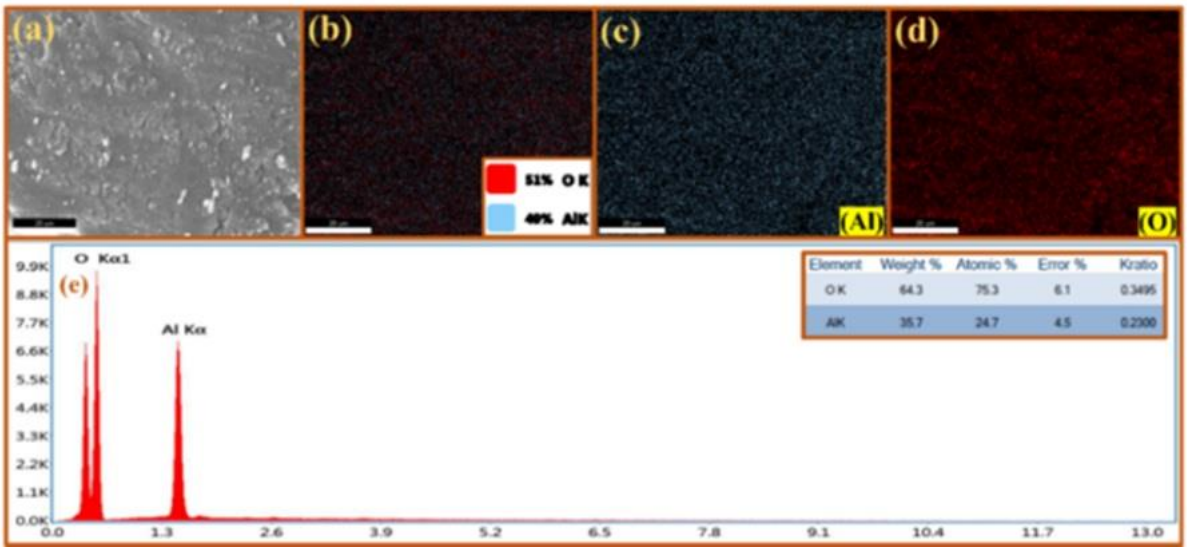

Figure 5. (i)-(a-e):represents the mapping images and spectrum analysis of Al NPs

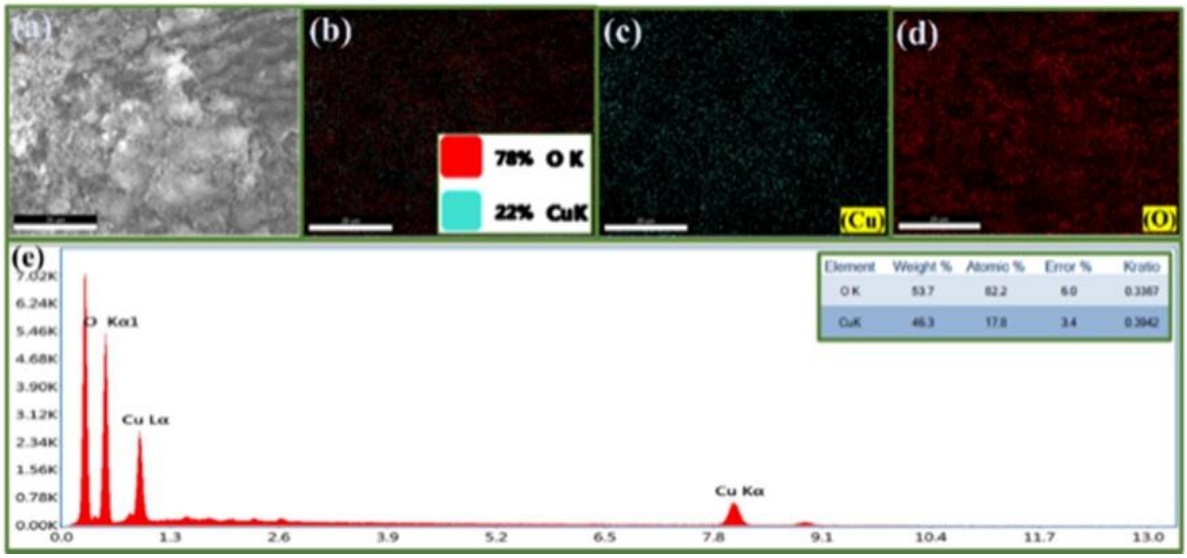

Figure 5. (ii)-(a-e):represents the mapping images and spectrum analysis of Cu NPs.

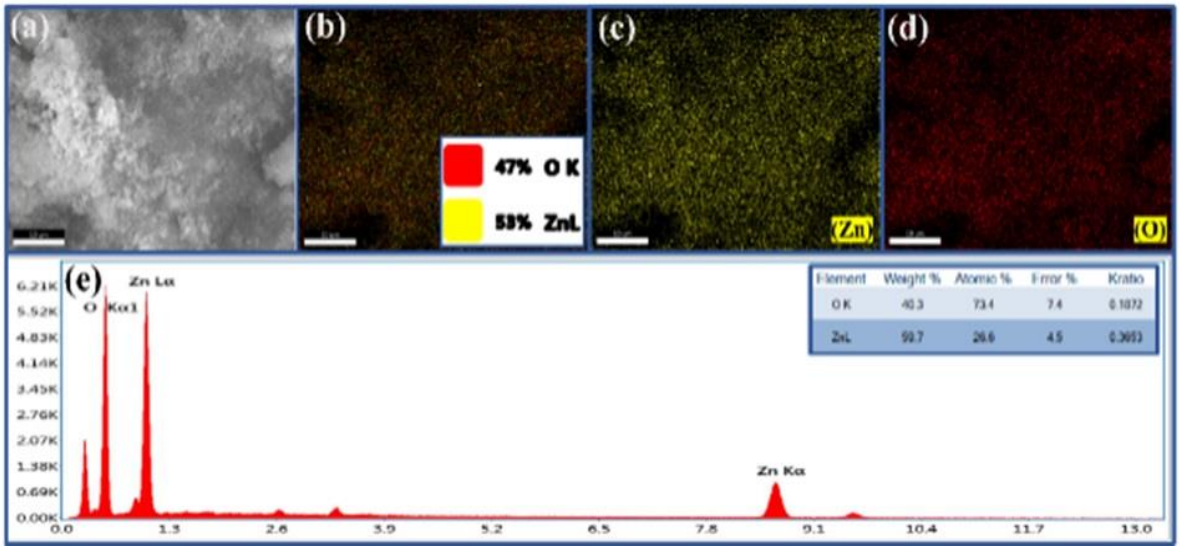

Figure 5. (iii)-(a-e):represents the mapping images and spectrum analysis of Zn NPs

3.6. Testing of Conductivity

The electrical conductivity was measured with an electrical conductivity meter [28]. The electrical conductance of Al NPs, Zn NPs, and Cu NPs, are 0.461, 1.616, and 2.6 S/m respectively. Here, copper has the highest conductance value. So, it can be used for the coating process in solar photovoltaic panels which will increase the photoelectric effect.

4. Conclusion

The green synthesis of metal NPs (Al, Cu, and Zn NPs) using a rosy periwinkle leaf extract offers a competitive alternative to more intricate chemical processes. The green synthesis technique is portrayed as a sustainable and versatile approach, offering benefits in terms of safety, cost-effectiveness, and reduced environmental impact. The characterization techniques such as UV-Vis, XRD, FTIR, SEM, and EDX helped confirm the crystalline structure, optical properties, functional groups, surface morphology, and elemental compositions, which were well-matched with the NPs. Hence, the synthesized NPs can be used for further applications. Electrical conductivity is a crucial factor in the performance of solar panels, as it influences the efficiency of electron transport within the panel. Hence, green synthesized NPs offer high electrical conductivity Thus, this research suggests that Cu NPs, Al NPs, and Zn NPs can enhance the electrical conductivity of metal coatings applied to solar panels. Overall, this research contributes valuable insights into the potential applications of green-synthesized metal NPs, particularly in the context of solar panel coatings. The environmentally friendly nature of the green synthesis approach is highlighted as a significant advantage in the field of nanotechnology.

In summary, our research has shed fresh light on the uses of pink periwinkle leaf extract in solar panel coating applications, namely in the synthesis of metal nanoparticles (NPs) made of silver, gold, and platinum. As a result, employing rose periwinkle leaf extracts makes it feasible to suggest an environmentally friendly method of creating NPs. For coating applications in photovoltaic solar panels, it may be helpful. In the realm of nanotechnology, the green synthesis technique is a quick, inexpensive, and environmentally beneficial procedure.Metal nanoparticles made from plants are safer, more scalable, and more stable.

References

[1] Mitarotonda, Romina, Martín Saraceno, Marcos Todone, Exequiel Giorgi, Emilio L Malchiodi, Martín F Desimone, and Mauricio C De Marzi, “Surface Chemistry Modification of Silica Nanoparticles Alters the Activation of Monocytes.” Therapeutic Delivery 12 (6), 2021, pp. 443–59. https://doi.org/10.4155/tde-2021-0006.

[2] Sharafi, Mahdi, and Hamid Oveisi. "A high-performance perovskite solar cell with a designed nanoarchitecture and modified mesoporous titania electron transport layer by zinc nanoparticles impurity." Materials Science and Engineering: B 296, 2023, 116608. https://doi.org/10.1016/j.mseb.2023.116608.

[3] Balkrishna, Acharya, Naveen Thakur, Bhavana Patial, Saurabh Sharma, Ashwani Kumar, Vedpriya Arya, and Ryszard Amarowicz. "Synthesis, characterization and antibacterial efficacy of Catharanthus roseus and Ocimum tenuiflorum-mediated silver nanoparticles: phytonanotechnology in disease management." Processes, 11, no.5, 2023, pp.1479. https://doi.org/10.3390/pr11051479.

[4] Husen, Azamal, ed. Secondary metabolites-based green synthesis of nanomaterials and their applications. Springer, 2023.http://dx.doi.org/10.1007/978-981-99-0927-8

[5] Vijayaram, Seerengaraj, Hary Razafindralambo, Yun-Zhang Sun, Seerangaraj Vasantharaj, Hamed Ghafarifarsani, Seyed Hossein Hoseinifar, and Mahdieh Raeeszadeh. "Applications of green synthesized metal nanoparticles—a review." Biological Trace Element Research 202, no. 1, 2024, pp.360-386. https://doi.org/10.1007/s12011-023-03645-9.

[6] Rajeshkumar, Shanmugam, Royapuram Parthasarathy Parameswari, Dayalan Sandhiya, Khalid A. Al-Ghanim, Marcello Nicoletti, and Marimuthu Govindarajan. "Green synthesis, characterization and bioactivity of Mangifera indica seed-wrapped zinc oxide nanoparticles." Molecules 28, no. 6, 2023, pp. 2818. https://doi.org/10.3390/molecules28062818.

[7] Diao, Fa-Ming, Man-Li Chen, Lin-Yin Tong, Ying-Nan Chen, and Zeng-Hui Diao. "A green synthesized medicine residue carbon-based iron composite for the removal of chromium (VI) and cadmium (II): Performance, kinetics and mechanism." Environmental Science and Pollution Research 30, no. 35, 2023, pp.84011-84022. https://doi.org/10.1007/s11356-023-28429-5.

[8] Khan, Salim, Fahad Al-Qurainy, Abdulrahman Al-Hashimi, Mohammad Nadeem, Mohamed Tarroum, Hassan O. Shaikhaldein, and Abdalrhaman M. Salih. "Effect of green synthesized ZnO-NPs on growth, antioxidant system response and bioactive compound accumulation in Echinops macrochaetus, a potential medicinal plant, and assessment of genome size (2C DNA content)." Plants 12, no. 8, 2023, pp.1669. https://doi.org/10.3390/plants12081669.

[9] Manojkumar, Utaiyachandran, Durairaj Kaliannan, Venkatesan Srinivasan, Balamuralikrishnan Balasubramanian, Hesam Kamyab, Zainab Haider Mussa, Jayanthi Palaniyappan, Mohsen Mesbah, Shreeshivadasan Chelliapan, and Senthilkumar Palaninaicker. "Green synthesis of zinc oxide nanoparticles using Brassica oleracea var. botrytis leaf extract: Photocatalytic, antimicrobial and larvicidal activity." Chemosphere 323, 2023, pp.138263. https://doi.org/10.1016/j.chemosphere.2023.138263.

[10] Ali, Noor Al-Huda R., and Majid H. Hassouni. "Effective (Cuo) Nanoparticles with Crocus Sativus Prepared by Green Synthesis of S. Aureus and S. Epidermidis Activity." HIV Nursing 23, no. 3, 2023, pp.2003-2008.https://doi.org/10.31838/hiv23.03.299

[11] Kabiriyel, J., R. Jeyanthi, K. Jayakumar, Augustine Amalraj, P. Arjun, A. Shanmugarathinam, G. Vignesh, and C. Raja Mohan. "Green synthesis of carboxy methyl chitosan based curcumin nanoparticles and its biological activity: Influence of size and conductivity." Carbohydrate Polymer Technologies and Applications 5, 2023, pp. 100260. https://doi.org/10.1016/j.carpta.2022.100260.

[12] Suárez-Cerda, Javier, Heriberto Espinoza-Gómez, Gabriel Alonso-Núñez, Ignacio A. Rivero, Yadira Gochi-Ponce, and Lucía Z. Flores-López. "A green synthesis of copper nanoparticles using native cyclodextrins as stabilizing agents." Journal of Saudi Chemical Society 21, no. 3, 2017, pp.341-348. https://doi.org/10.1016/j.jscs.2016.10.005.

[13] Mehta, B. K., Meenal Chhajlani, and B. D. Shrivastava. "Green synthesis of silver nanoparticles and their characterization by XRD." In Journal of physics: conference series, vol. 836, no. 1, p. 012050. IOP Publishing, 2017. https://doi :10.1088/1742-6596/836/1/012050

[14] Sharma, Jitendra Kumar, M. Shaheer Akhtar, S. Ameen, Pratibha Srivastava, and Gurdip Singh. "Green synthesis of CuO nanoparticles with leaf extract of Calotropis gigantea and

its dye-sensitized solar cells applications." Journal of Alloys and Compounds 632, 2015, pp.321-325. https://doi.org/10.1016/j.jallcom.2015.01.172.

[15] Vidya, C., Shilpa Hiremath, M. N. Chandraprabha, M. L. Antonyraj, Indu Venu Gopal, Aayushi Jain, and Kokil Bansal. "Green synthesis of ZnO nanoparticles by Calotropis gigantea." Int J Curr Eng Technol 1, no. 1, 2013, pp.118-120. https:// 10.1007/s10854-017-7254-2

[16] Malik, Azad Qayoom, Tahir ul Gani Mir, Deepak Kumar, Irtiqa Ashraf Mir, Adfar Rashid, Mehnaz Ayoub, and Saurabh Shukla. "A review on the green synthesis of nanoparticles, their biological applications, and photocatalytic efficiency against environmental toxins." Environmental Science and Pollution Research 30, no. 27, 2023, pp. 69796-69823. https://doi.org/10.1007/s11356-023-27437-9.

[17] Al-Azzawi, Marwa A., Wasan R. Saleh, Farqad Abdullah Rashid, and Bushra MJ Alwash. "Synthesis and Characterization of Nanoparticles Extracted from Catharanthus roseus Plant." Nano Hybrids and Composites 38, 2023, pp.15-24.https://doi.org/10.4028/p-z7zy4l.

[18] Tiwari, Anand D., Ajay K. Mishra, Shivani B. Mishra, Alex T. Kuvarega, and Bhekie B. Mamba. "Stabilisation of silver and copper nanoparticles in a chemically modified chitosan matrix." Carbohydrate polymers 92, no. 2, 2013, pp.1402-1407. https://doi.org/10.1016/j.carbpol.2012.10.008.

[19] Abdulwahab, F., F. Z. Henari, S. Cassidy, and K. Winser. "Synthesis of Au, Ag, Curcumin Au/Ag, and Au-Ag Nanoparticles and Their Nonlinear Refractive Index Properties." Journal of Nanomaterials 2016, no. 1, 2016, pp.5356404. https://doi.org/10.1155/2016/5356404.

[20] Alhalili, Zahrah. "Green synthesis of copper oxide nanoparticles CuO NPs from Eucalyptus Globoulus leaf extract: Adsorption and design of experiments." Arabian Journal of Chemistry 15, no. 5, 2022, pp.103739. https://doi.org/10.1016/j.arabjc.2022.103739.

[21] Amargeetha, A., and S. Velavan. "X-ray diffraction (XRD) and energy dispersive spectroscopy (EDS) analysis of silver nanoparticles synthesized from Erythrina indica flowers." Nanosci. Technol. Open Access 5, 2018, pp.1-5https://:10.15226/2374-8141/5/1/00152.

[22] Ibrahim Dincer " Hydrogen and Fuel Cell Technologies for Sustainable Future", Jordan Journal of Mechanical and Industrial Engineering, Volume 2, Number 1, Mar. 2008 ISSN 1995-6665 Pages 1 – 14https://10.3390/en12234593

[23] Al-Ghandoor ,J.O. Jaber ,and I. Al-Hinti's "Assessment of Energy and Exergy Efficiencies of Power Generation Sub-Sector" Jordan Journal of Mechanical and Industrial Engineering, Volume 3, Number 1, March. 2009 ISSN 1995-6665 Pages 1 – 8.https://doi.org/10.1166/asem.2013.1242.

[24] Kasim M. Daws, Zouhair I. AL-Dawood, Sadiq H. AL-KabiFuzzy "Logic Approach for Metal Casting Selection Process" Jordan Journal of Mechanical and Industrial Engineering, Volume 3, Number 3, September 2009 ISSN 1995-6665 Pages 162 – 167 https://10.4271/2003-01-0431

[25] Renna "Dynamic Control Card in a Production System Controlled by Conwip Approach Paolo",Jordan Journal of Mechanical and Industrial Engineering, Volume 4, Number 4, September 2010 ISSN 1995-6665 Pages 425 – 432 https://10.1016/j.ijpe.2004.12.010

[26] K. Tiwari, R.K. Singh, B. Kumar, "Optimizing PM Intervals for Manufacturing Industries Using Delay-time Analysis and MOGA" Jordan Journal of Mechanical and Industrial Engineering, Volume 16, Number 3, June. 2022 ISSN 1995-6665 Pages 327 – 332. https://doi.org/10.1166/asem.2013.1242

[27] J.O. Jaber, "Prospects and Challenges of Small Hydropower Development", Jordan Journal of Mechanical and Industrial Engineering, Volume 6, Number 2, April 2012 ISSN 995-6665 Pages 110 - 118.https://10.4271/2003-01-031.

[28] Raed Al-Rbaihat, Ahmad Sakhriehb, Jamil Al-Asfar Ali Alahmer, Osama Ayadi, Ahmed Al-Salaymeh, Zayed Al_hamamre, Abeer Al-bawwab, Mohammed Hamdan Combined Solar-Geothermal Power Generation using Organic Rankine Cycle Volume 11 Number 1, January. 2017 ISSN 1995-6665 Pages 1 -11. https://doi.org/10.3390/molecules28020808.